International Journal of Mechanical, Industrial and Aerospace Sciences
ISSN: 2517-9950
Vol:7, No:8, 2013

Transient Population Dynamics of Phase Singularities in 2D Beeler-Reuter Model

Hidetoshi Konno and Akio Suzuki

Abstract—The paper presented a transient population dynamics of phase singularities in 2D Beeler-Reuter model. Two stochastic modelings are examined: (i) the Master equation approach with the transition rate (i.e., $\lambda(n,t) = \lambda(t)n$ and $\mu(n,t) = \mu(t)n$) and (ii) the nonlinear Langevin equation approach with a multiplicative noise. The exact general solution of the Master equation with arbitrary time-dependent transition rate is given. Then, the exact solution of the mean field equation for the nonlinear Langevin equation is also given. It is demonstrated that transient population dynamics is successfully identified by the generalized Logistic equation with fractional higher order nonlinear term. It is also demonstrated the necessity of introducing time-dependent transition rate in the master equation approach to incorporate the effect of nonlinearity.

Keywords—Transient population dynamics, Phase singularity, Birth-death process, Non-stationary Master equation, nonlinear Langevin equation, generalized Logistic equation.

I. Introduction

Many researcher's attentions have been payed for the study of *spiral wave formations* and *spiral wave turbulence* (SWT) [1] in conjunction with a problem of the ventricular fibrillation (VF) – an origin of the sudden death. Although large scale 3D simulations have been performed all over the world, they do not succeed fully in describing them from the view points of physics, mathematics and physiology.

In our previous paper [2], the 2D Aliev-Panfilov (AP) model [3] is studied since the model can exhibit the SWT. Among many physical state variables in characterizing the SWT, we choose the phase singularity (PS) as a key quantity to describe the state of the SWT. The PS is important since it plays as the wave source even in broken pieces of spiral waves. Actually, the finite-time local Lyapunov exponent take large value along the line connecting the PS. It is found [2] that the number of PSs can be described well by the Gamma process at the steady state. The stochastic Logistic equation with a multiplicative noise can mimic the dynamical features of the fluctuation of the number of PSs at the steady state.

To examine the universality of the result in the AP model, we have examined [4] the 2D Beeler-Reuter (BR) [5] model where many ion channels are taken into account [cf. Appendix A]. With the use of the BR model, one can discuss the physical and physiological significance of the transitions of state from the normal to states of heart diseases like VF. Extensive numerical simulations are performed by changing the parameters and the system size of the BR model. It is found that the fluctuation of the number of PSs in the BR model [cf. Appendix B for the method of detecting PS] is subjected to the hyper Gamma process described by [4,6]

$$\frac{d}{dt}N = aN - bN^m + NF(t) \ , \tag{1}$$

where the random force $F(t)$ is assumed to be a Gaussian-white noise with null mean: $\langle F(t)\rangle = 0$ and $\langle F(t)F(t')\rangle = 2D\delta(t-t')$, with a fractional nonlinearity m, and a and b are assumed to be positive constants. The noise correction is accounted provided that eq.(1) is a Stratonivich type SDE ($a \to a + D$). At the steady state, the model gives the hyper Gamma (HG) distribution in the form:

$$P(X) = \frac{\alpha\beta^{\frac{\gamma}{\alpha}}}{\Gamma(\frac{\gamma}{\alpha})}X^{\gamma-1}\exp(-\beta X^{\alpha}), \tag{2}$$

where $\Gamma(z)$ is the Gamma function. The parameters of distribution in eq.(2) and those of the Langevin equation in eq.(1) are related as

$$\alpha = m-1, \beta = \frac{b}{D(m-1)} \ \text{ and } \ \gamma = \frac{a}{D} \ . \tag{3}$$

In this case, there are different parameter regions that the nonlinearity m change depending on the parameters and the size of the system.

In spite of the success to mimic the stochastic time evolution of the number of phase singularities at the steady-state, the performance of description based on the stochastic hyper Gamma process is not validated for the non-stationary nature of initial transient from a single spiral to a state of SWT.

In this paper, two non-stationary birth-death processes are examined: (a) the Master equation approach and (b) the Langevin equation approach. The paper is organized as follows. Section II introduces the Master equation approach with time-dependent birth-death rates under the fixed initial condition. The exact analytic solution of it for different birth and death rates of time-dependent functions is given. The expressions of the mean and the variance are also given. Section III introduces the Langevin equation approach with eq.(1) under the fixed initial condition. Section IV discusses on the results of two different approaches. The last section is devoted to summary and remarks.

II. Master Equation Approach

A. Master Equation

Consider a generalized non-stationary birth-death process in the form of the Master equation:

$$\frac{d}{dt}p(n,t) = \lambda(n-1,t)p(n-1,t) + \mu(n+1,t)p(n+1,t)$$

H. Konno is with the Department of Risk Engineering, Faculty of Information and Systems, University of Tsukuba, Tsukuba, Tsukuba, Ibaraki 305-8573 JAPAN(e-mail: konno.hidetoshi.fu@u.tsukuba.ac.jp).

A. Suzuki is with National Institute of Advanced Industrial Science and Technology, Tsukuba, Ibaraki 305-8564 Japan(e-mail: akio.suzuki@aist.go.jp).

$$-[\lambda(n,t)+\mu(n,t)]p(n,t)\ ,(n\geq 1) \tag{4}$$

where the transition rates are assumed simply proportional to the state n (or the number of state)

$$\lambda(n,t)=\lambda(t)n \ \text{ and } \ \mu(n,t)=\mu(t)n. \tag{5}$$

$\lambda(t)$ and $\mu(t)$ are arbitrary functions with time. These functions $\lambda(t)$ and $\mu(t)$ represent the memory in the system. For $n=0$, $dp(0,t)/dt=\mu(1,t)p(1,t)$. Since the birth and the death rate in eq.(5) are assumed, the condition $n\geq 1$ must be imposed in eq.(4). Also, the initial condition is assumed to have $p(n,0)=\delta_{n,n_0}$ with $n_0\geq 1$.

B. Generating function

The generating function $g(z,t)$ defined by $g(z,t)=\sum_{n=0}^{\infty}z^n p(n,t)$ for eq.(4) with the transition rates in eq.(5) obeys

$$\frac{d}{dt}g(z,t)=(\lambda(t)z-\mu(t))(z-1)\frac{\partial}{\partial z}g(z,t)\ . \tag{6}$$

From the initial condition, $g(z,0)=z^{n_0}$. This is a partial differential equation of the variable coefficients $\lambda(t)$ and $\mu(t)$. To solve this equation, let us consider the auxiliary equation,

$$\frac{dt}{1}=-\frac{dz}{(\lambda(t)z-\mu(t))(z-1)}=\frac{dg}{0}\ . \tag{7}$$

From the first equation, one obtains a nonlinear Riccati equation,

$$\frac{dz}{dt}=-(\lambda(t)z-\mu(t))(z-1)\ . \tag{8}$$

Since $z=1$ is one of the solution of the equation, it is readily seen that the variable transformation $\xi=(z-1)^{-1}$ (i.e., $z=1+\xi^{-1}$) leads eq.(8) to

$$\frac{d\xi}{dt}=(\lambda(t)-\mu(t))\xi+\lambda(t)\ . \tag{9}$$

This is a first order linear differential equation with the variable coefficients $\lambda(t)$ and $\mu(t)$. The general solution of eq.(9) is given by

$$\xi(t)=\exp([\Lambda(t)-M(t)])\left(\int_0^t\lambda(\tau)V(\tau)\ d\tau+C\right)\ , \tag{10}$$

where

$$\Lambda(t)=\int_0^t\lambda(\tau)\ d\tau \ \text{ and } \ M(t)=\int_0^t\mu(\tau)\ d\tau\ , \tag{11}$$

and

$$V(t)=\exp\left\{-[\Lambda(t)-M(t)]\right\}V(0)\ . \tag{12}$$

Therefore, the equation (10) is written in the form:

$$\xi(t)V(t)-W(t)=C\ , \tag{13}$$

where

$$W(t)=\int_0^t\lambda(\tau)V(\tau)\ d\tau\ . \tag{14}$$

It is readily see that the solution of eq.(6) is given by

$$g(z,t)=f\left(\frac{V(t)}{z-1}-W(t)\right)\ . \tag{15}$$

Actually, substituting eq.(15) into eq.(6), one obtains the balancing equations for $V(t)$ and $W(t)$ as $\dot{V}(t)=-(\lambda(t)-\mu(t))V(t)$ and $\dot{W}(t)=\lambda(t)V(t)$ with $V(0)=1$ and $W(0)=0$.

From the initial condition $f\left(\frac{1}{z-1}\right)=z^{n_0}$, the form of $f(x)$ is determined as

$$f(x)=\left(\frac{1+x}{x}\right)^{n_0}\ . \tag{16}$$

The generating function is expressed as

$$g(z,t)=\left\{\frac{[1-W(t)]z+V(t)+W(t)-1}{V(t)+W(t)-W(t)z}\right\}^{n_0}\ , \tag{17}$$

$$=\left\{\frac{[1-W(t)]z+V(t)+W(t)-1}{V(t)+W(t)}\times\sum_{n=0}^{\infty}\left(\frac{W(t)}{V(t)+W(t)}z\right)^n\right\}^{n_0}\ . \tag{18}$$

C. Probability Mass function

For $n_0=1$, one obtains the simple expression of the probability mass function (pmf) $p(n,t)$ in the form:

$$p(0,t)=1-\frac{1}{V(t)+W(t)}\ (n=0) \tag{19}$$

and

$$p(n,t)=\frac{(W(t))^{n-1}V(t)}{(V(t)+W(t))^{n+1}}\ (n\geq 1)\ . \tag{20}$$

It is easy to show that $\sum_{n=1}^{\infty}p(n,t)=1/(V(t)+W(t))$ and $\sum_{n=0}^{\infty}p(n,t)=1$.

When there is no memory, i.e.,

$$\lambda(t)=\lambda \ \text{ and } \ \mu(t)=\mu\ , \tag{21}$$

the probability mass function reduces to

$$p(0,t)=\frac{\mu\theta}{\lambda}\ (n=0) \tag{22}$$

and

$$p(n,t)=\frac{1}{\lambda}(1-\theta)(\lambda-\mu\theta)\theta^{n-1}\ (n\geq 1)\ , \tag{23}$$

where

$$\theta=\frac{\lambda(\exp[(\lambda-\mu)t]-1)}{\lambda\exp[(\lambda-\mu)t]-\mu}\ . \tag{24}$$

It is easy to show that $\sum_{n=1}^{\infty}p(n,t)=\frac{(\lambda-\mu\theta)}{\lambda}$ and $\sum_{n=0}^{\infty}p(n,t)=1$.

D. Mean and variance

The general expressions of the mean, the variance and the Fano factor (the variance-to-mean ratio) in terms of $V(t)$ and $W(t)$ in eqs.(13) and (14) are

$$\langle n(t)\rangle=\frac{1}{V(t)}\ , \tag{25}$$

$$\sigma_n^2(t)=\frac{1}{V(t)}\left[\frac{2W(t)+V(t)-1}{V(t)}\right] \tag{26}$$

and

$$F(t) = \frac{\sigma_n^2(t)}{\langle n(t)\rangle} = \left[\frac{2W(t) + V(t) - 1}{V(t)}\right] . \quad (27)$$

Since the pmf is classified into the asymmetric time-dependent function, the third moment is obtained as

$$\langle n(t)^3\rangle = 6\frac{W(t)^2}{V(t)^3} + 6\frac{W(t)}{V(t)^2} - 2\frac{1}{V(t)} . \quad (28)$$

In the case of no memory (i.e, λ and μ are constants) in eq.(20) , the expressions (24)-(25) reduces to

$$\langle n(t)\rangle = \frac{\lambda - \mu\theta}{\lambda(1-\theta)} \quad (29)$$

and

$$\sigma_n^2(t) = \frac{(\lambda+\mu)(\lambda-\mu\theta)\theta}{\lambda^2(1-\theta)^2} , \quad (30)$$

where θ is defined in eq.(24). The mean, the variance and the Fano factor are expressed in the simplified forms:

$$\langle n(t)\rangle = \exp\left\{(\lambda-\mu)t\right\} , \quad (31)$$

$$\sigma_n^2(t) = \left(\frac{\lambda+\mu}{\lambda-\mu}\right)\exp\left\{(\lambda-\mu)t\right\}\left[\exp\left\{(\lambda-\mu)t\right\} - 1\right] \quad (32)$$

and

$$F(t) = \left(\frac{\lambda+\mu}{\lambda-\mu}\right)\left[\exp\left\{(\lambda-\mu)t\right\} - 1\right] . \quad (33)$$

They exhibit the exponential growth for $\lambda > \mu$ for the case of constant rate ((i) in Table I: Markovian case, the case without memory).

E. Simple Mathematical Examples for $\lambda(t)$ and $\mu(t)$

Some simple mathematical examples of time-dependent function $\lambda(t)$ and $\mu(t)$ are listed in Table I. These are increasing/decreasing functions of time. The cases of (i) the constant rate, (ii) the linear time-dependent growth rate, (iii) the exponential growth ($\gamma_j < 0$)/relaxation ($\gamma_j > 0$) ($j = \lambda, \mu$), (iv) the inverse power relaxation function, and (v) the power growth ($\gamma_j > 1$)/relaxation ($\gamma_j < 1$) ($j = \lambda, \mu$). In the case of the generalized Polya process [7,8] (a class of the birth process) in eq.(1), only the time-dependent birth rate $\lambda(t)$ is accounted. In this case, the inverse power function (iv) has been used in the applications to the problems of infectious disease [8] in the demography and of after shock in the seismology [9].

In the birth-death process in eq.(4), there are various combinations of different increasing/decreasing functions of $\lambda(t)$ and $\mu(t)$ other than Table I.

Table I: Simple functions of $\lambda(t)$ and $\mu(t)$

	$\lambda(t)$	$\mu(t)$
(i)	λ	μ
(ii)	λt	μt
(iii)	$\lambda\exp(-\gamma_\lambda t)$	$\mu\exp(-\gamma_\mu t)$
(iv)	$\frac{\lambda}{1+\gamma_\lambda t}$	$\frac{\mu}{1+\gamma_\mu t}$
(v)	$\lambda t^{\gamma_\lambda - 1}$	$\mu t^{\gamma_\mu - 1}$

Let us exhibit some simple examples of the mean evolution $\langle n(t)\rangle$ provided that $\gamma_\lambda = \gamma_\mu = \gamma \neq 0$: e.g.,
(ii) Gaussian growth/decay

$$\langle n(t)\rangle = \exp\left(\frac{1}{2}(\lambda-\mu)t^2\right) , \quad (34)$$

(iii) Double exponential function

$$\langle n(t)\rangle = \exp\left(\frac{1}{\gamma}(\lambda-\mu)[1-\exp(-\gamma t)]\right) , \quad (35)$$

(iv) Power growth/decay

$$\langle n(t)\rangle = (1+\gamma t)^{(\lambda-\mu)} \quad (36)$$

and
(v) Exponential growth/decay with fractional power of time

$$\langle n(t)\rangle = \exp\left(\frac{1}{\gamma}(\lambda-\mu)t^\gamma\right) . \quad (37)$$

III. Langevin Approach

As is shown in our previous paper [4], it is a convenient method to characterize the dynamics of ventricular fibrillation by detecting the number of phase singularity (PS). It is an interesting observation that the stochastic process of the number $N(t)$ of PSs in the steady is described well by the Langevin equation in stead of the above Master equation. Namely, the environmental fluctuation (i.e., the mutiplicative noise) is important. We can rewrite the Langevin equation in eq.(1) into the form:

$$\frac{d}{dt}N = \frac{k}{r}N\left[1 - \left(\frac{N}{K}\right)^r\right] + NF(t) . \quad (38)$$

where k, K and r are positive real constants. It is assumed that the noise correction is already done in the Langevin equation in eq.(38). The nonlinear structure is the same as the one ($m = 1 + r$) involved in the Langevin equation.

In the limit $r \to 0$, the above equation reduces to the stochastic Gompertz equation with the multiplicative noise $F(t)$:

$$\frac{d}{dt}N = -kN\ln(N/K) + NF(t) . \quad (39)$$

This is an interesting observation that the model gives the log-normal distribution at the steady state:

$$P_s(N) = \frac{1}{\sqrt{2\pi D/kN}}\exp\left(-\frac{(\ln(N) - \ln(K))}{2D/k}\right) . \quad (40)$$

When the mean field approximation is applied to the Langevin equation in eq.(38), one obtains

$$\frac{d}{dt}\langle N\rangle = \frac{k}{r}\langle N\rangle(1 - \langle(N/K)\rangle^r) . \quad (41)$$

The exact solution of eq.(41) is obtained in the form:

$$\langle N(t)\rangle = K\left[1 + \left\{\left(\frac{K}{N(0)}\right) - 1\right\}e^{-kt}\right]^{-\frac{1}{r}} . \quad (42)$$

In the limit $r \to 0$, this reduces to the solution of the Gompertz equation:

$$\langle N(t)\rangle = K\exp\left[\ln\left(\frac{N(0)}{K}\right)e^{-kt}\right] . \quad (43)$$

Let us remind here that the estimated values fractional order of nonlinearity m (or r) from our numerical experiments for Beeler-Reuter model are distributed in the range

$$1.5 < m < 4 \quad (0.5 < r < 3). \quad (44)$$

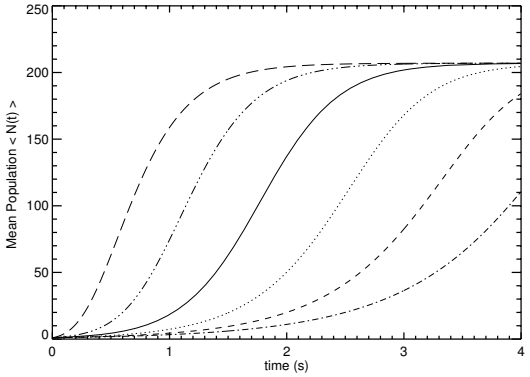

Fig. 1. Theoretical evolutions of a generalized Logistic equation with $K = 207$, $k = 3.0$ and $N(0) = 1$ are depicted: (a) long dased-line $r = 0$, (b) dash three-dots line $r = 0.5$, (c) solid line $r = 1$, (d) dotted line $r = 1.5$, (e) dashed line $r = 2.0$, (f) dash-dot line $r = 2.5$

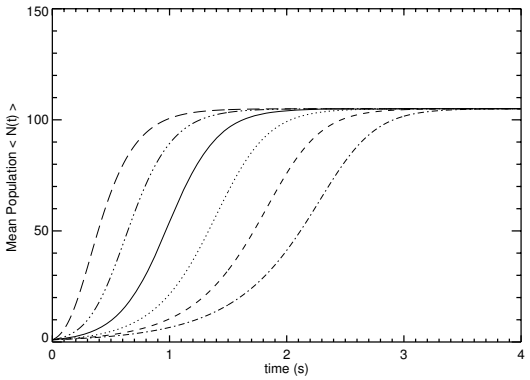

Fig. 2. Theoretical evolutions of a generalized Logistic equation with $K = 105$, $k = 4.7$ and $N(0) = 1$ are depicted: (a) long dased-line $r = 0$, (b) dash three-dots line $r = 0.5$, (c) solid line $r = 1$, (d) dotted line $r = 1.5$, (e) dashed line $r = 2.0$, (f) dash-dot line $r = 2.5$

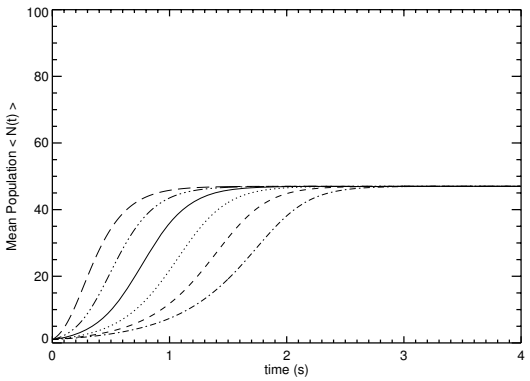

Fig. 3. Theoretical time evolution of a generalized Logistic equation with $K = 47$, $k = 5.0$ and $N(0) = 1$ are depicted: (a) long dased-line $r = 0$, (b) dash three-dots line $r = 0.5$, (c) solid line $r = 1$, (d) dotted line $r = 1.5$, (e) dashed line $r = 2.0$, (f) dash-dot line $r = 2.5$

Figures 1,2 and 3 show the transient mean time evolutions of the generalized Logistic equation are depicted in as a function of the value of the fractional order nonlinearity r for three values of K, i.e., $K = 47$, $K = 105$ and $K = 207$. The feature of time evolution in the Gompertz limit ($r = 0$) is also displayed. One can understand the r dependence on the population growth in the generalized Logistic equation.

IV. Results and Discussions

A. Identification by Generalized Logistic Equation

The method of numerical simulation in 2D Beeler-Reuter model with the parameters are described in detail in our previous paper [4]. To have fine statistical accuracy, we have adopted numerical simulation with a larger system size $L = 25$ cm in a transient situation that is started from a single spiral to a state of spiral wave turbulence. The number of phase singularity is counted in each time step in 2D space as described in our previous paper. The mean evolution is obtained by averaging over 6 set of sample data. Then, the population dynamics of phase singularities is identified by using the exact solution of the generalized Logistic equation. The time series data for the conductance values $g_s = 0.03$, $g_s = 0.07$ and $g_s = 0.09$ with system size $L = 25$ cm are utilized.

Figure 4 shows the mean population dynamics of phase singularities for $g_s = 0.03$ with the solid line. The dynamics is identified by the generalized Logistic equation with $r = 1$ ($m = 2$) in dash-dot line, which is consistent with the estimated value ($\hat{m} = 1.88$ [4]) at the steady state.

Figure 5 shows the mean population dynamics of phase singularities for $g_s = 0.07$ with the solid line. The dynamics is identified by the generalized Logistic equation with $r = 1.47$ ($m = 2.47$) in dash-dot line, which is consistent with the estimated value ($\hat{m} = 1.85$ [4]) at the steady state.

Figure 6 shows the mean population dynamics of phase singularities for $g_s = 0.09$ with the solid line. The dynamics is identified by the generalized Logistic equation with $r = 1.7$ ($m = 2.7$) in dash-dot line, which is consistent with the estimated value ($\hat{m} = 3.71$ [4]) at the steady state.

The successful identifiability with the use of the stochastic hyper Gamma process in both at (a) transient and (b) steady-state implies that the order of nonlinearity is physically significant for the understanding physical mechanism in the system. The results are summarized in Table II.

Table II: Estimated values of r and k

g_s	r	k	
(i) 0.03	1.0	3.0	Fig.4
(ii) 0.07	1.47	4.7	Fig.5
(iii) 0.09	1.7	5.0	Fig.6

B. Incorporation of Nonlinearity in the Master Equation

Nonlinear dynamics of spiral wave turbulence (SWT) has been studied extensively in conjunction the ventricular fibrillation (VF) by using various models of heart [1]. It is expected from observations of numerical results that the state of SWT

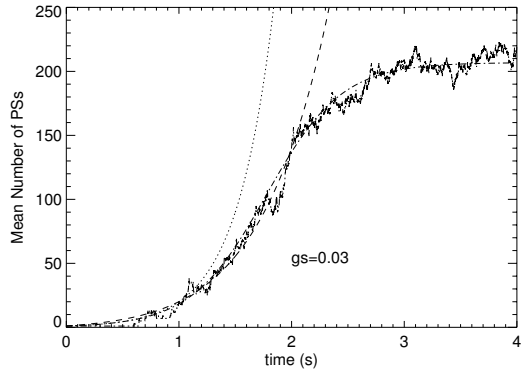

Fig. 4. Time evolution of the mean number of phase singularities for the conductance $g_s = 0.03$ in the Beeler-Reuter model. Six sets of sample data are averaged to obtain it. The mean time evolution of a generalized Logistic equation for $r = 1.0$ is also shown with dashed line. The dotted line indicates the result of identification by the non-stationary birth-death process with an exponential growth of fractional time $\exp(\epsilon t^{\gamma})$ with $\epsilon = 3.0$ and $\gamma = 0.72$.

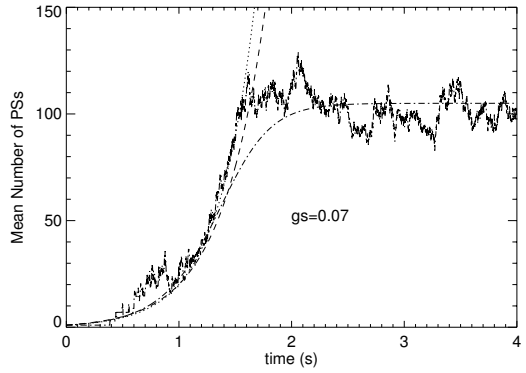

Fig. 5. Time evolution of the mean number of phase singularities for the conductance $g_s = 0.07$ in the Beeler-Reuter model. Six sets of sample data are averaged to obtain it. The time evolution of a generalized Logistic equation for $r = 1.47$ is also shown with dashed-line. The dotted line indicates the result of identification by the non-stationary birth-death process with an exponential growth of fractional time $\exp(\epsilon t^{\gamma})$ with $\epsilon = 3.0$ and $\gamma = 0.9$.

(VF) is characterized by the interactions of phase singularities:

$$2X \rightarrow^{k_1} X \text{ (wave merge) },$$

$$X \rightarrow^{k_2} 2X \text{ (wave break) },$$

$$X \rightarrow^{k_3} 0 \text{ (death and/or loss from the region)}$$

and

$$2X \rightarrow^{k_4} 0 \text{ (pair extinction).}$$

This interaction scheme is identical with the Schlögl's first model in chemical reaction [10]. The model is described in terms of the Master equation:

$$\frac{d}{dt}P(X,t) = k_1(X+1)XP(X+1,t)$$
$$+k_2(X-1)P(X-1,t) + k_3(X+1)P(X+1,t)$$
$$+k_4(X+2)(X+1)P(X+2,t) - k_1X(X-1)P(X,t)$$

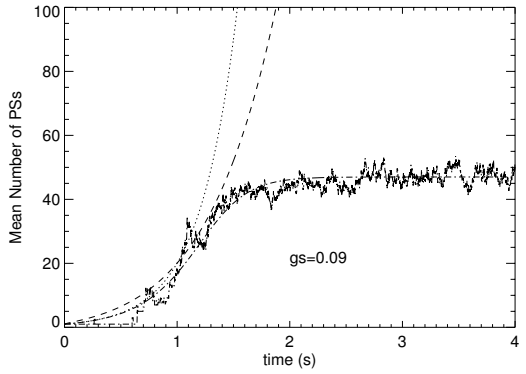

Fig. 6. Time evolution of the mean number of phase singularities for the conductance $g_s = 0.09$ in the Beeler-Reuter model. Six sets of sample data are averaged to obtain it. The time evolution of a generalized Logistic equation for $r = 1.7$ is also shown with dashed-line. The dotted line indicates the result of identification by the non-stationary birth-death process with an exponential growth of fractional time $\exp(\epsilon t^{\gamma})$ with $\epsilon = 3.0$ and $\gamma = 0.68$.

$$-(k_2+k_3)XP(X,t) - k_4X(X-1)P(X,t) \ . \qquad (45)$$

The equation of the mean is derived from the Master equation as

$$\frac{d}{dt}\langle X\rangle = a\langle X\rangle - b\langle X^2\rangle \qquad (46)$$

with

$$a = (k_1 + k_2 - k_3 + 2k_4) \ \text{ and } \ b = (k_1 + 2k_4). \qquad (47)$$

Under the mean field approximation $\langle X^2\rangle \approx \langle X\rangle^2$, the Logistic equation is obtained. However, one can not get higher order nonlinearity within the interaction schemes described above (cf. the interaction mechanisms discussed in Refs. [11],[12] and [13]). Also, the origin of the environmental fluctuation (i.e., the multiplicative noise) can not be derived within the framework of the Master equation with a single variable X.

However, one can not get higher order nonlinearity within the interaction schemes described above. Also, the origin of the environmental fluctuation (i.e., the multiplicative noise) can not be incorporated within the framework of the Master equation with a single variable X. Although Gillespie's algorithm [14] can be utilized to perform direct simulation of the Master equation is possible, the inverse problem to infer the reaction rates of interactions is not easy.

C. Identification of time-dependent Birth-Death rates

As is explained in the previous subsection, the analytical treatment of the master equation approach with incorporating nonlinear terms is not easy. Therefore, the phenomenological treatment with the use of the time-dependent birth-death rate may be available.

When the Markovian description is adopted, i.e., $\lambda(t) = \lambda$ and $\mu(t) = \mu$, the exponential growth is expected as shown in eq.(31). In this case, the time evolution is shown in the dotted line in Figs.4, 5 and 6. This simple exponential curve can reproduce only the curve of our numerical experiment in the initial part of the transient. To improve the Markovian

description, one must introduce a time-dependent function among the simple functions listed in Table I. It is easy to see that an appropriate choice is taking (v) a fractional power of time like

$$\lambda(t) = \lambda t^{\gamma-1} \quad \text{and} \quad \mu(t) = \mu t^{\gamma-1} \ . \tag{48}$$

The mean evolution can be improved by an exponential growth with a fractional power of time:

$$\langle N(t) \rangle = \exp\left(\epsilon t^{\gamma}\right) \ , \tag{49}$$

where $\epsilon = (\lambda - \mu)/\gamma$. As is shown with the dashed lines in Figs. 4, 5 and 6, the feature of evolution is improved from a simple exponential growth. The results are summarized in Table III. The introduction of nonlinear suppression is required for further improvement as shown with the generalized Logistic evolution.

Table III: Estimated values of ϵ and γ

g_s	ϵ	γ	
(i) 0.03	3.0	0.72	Fig.4
(ii) 0.07	3.0	0.9	Fig.5
(iii) 0.09	3.0	0.68	Fig.6

V. Conclusion

The paper presented a transient population dynamics of phase singularities in 2D Beeler-Reuter model. Two stochastic birth-death processes are examined based on (i) the Master equation in eq.(4) with the transition rate (i.e., $\lambda(n,t) = \lambda(t)n$ and $\mu(n,t) = \mu(t)n$) and (ii) the Langevin equation in eq.(1) with a multiplicative noise. The derivation of the exact general solution of eq.(4) is shown in section II. Then, the exact solution of the mean field equation for the Langevin equation in eq.(1) is given in section III. Transient population dynamics is successfully identified by the generalized Logistic equation in eq.(38) with fractional higher order nonlinear term in section IV. Interestingly, the estimated values [4] of the model parameters form transient population dynamics are consistent with those at the features of fluctuations at the steady state.

Appendix A
Beeler-Reuter model with DR modification

$$\frac{\partial V_m}{\partial t} = \mathcal{D}\nabla^2 V_m - \frac{I_{ion} - I_{st}}{C_m} \ , \tag{A1}$$

where V_m (mV) is transmembrane voltage, $\mathcal{D}$ ($\mathrm{cm}^2/\mathrm{ms}$) is the diffusion coefficient, C_m ($\mu\mathrm{F}/\mathrm{cm}^2$) is membrane capacitance, I_{ion} ($\mu\mathrm{A}/\mathrm{cm}^2$) is the sum of ionic transmembrane currents, I_{st} ($\mu\mathrm{A}/\mathrm{cm}^2$) is the stimulus current, and ∇^2 is the Laplacian in 2D space. Various modifications can be made for describing ionic currents. In this paper, the Drouhard-Roberge (DR) modification of the Beeler-Reuter (BR) cardiac cell model (BRDR model) is adopted, which is the simplest ionic model for mammalian ventricular tissue using four ionic currents, five ionic gates, and intracellular calcium concentration.

Numerical simulations of the BRDR model are performed in a 2D square domain $\Omega = [0, L] \times [0, L]$ ($L = 25$ cm) with Neumann (zero flux) boundary conditions. To reduce computation time, numerical integration is performed using a forward Euler scheme with a time step 0.025 ms. The Laplacian is discretized using a 9-point difference formula with a spatial mesh 0.025 cm. Space-time variations of state variables are stored with a time step of 1.0 ms and a space step 0.05 cm. In our simulations, the values of the two parameters $\mathcal{D} = 9.72 \times 10^{-4}$ and $C_m = 1.0$ are kept constant. The BRDR model parameter values of Ref.[5] are adopted in this study, except for the values of slow inward current conductance g_s ($\mathrm{mS}/\mathrm{cm}^2$).

Appendix B
Method for Detecting Phase Singularity

The phase singularity (PS) is identified as the local site where the phase is undefined. The PSs appear at the core of the rotating waves, and their existence is a necessary (but not a sufficient) condition for the occurrence of breaking waves. The position of a PS can be identified from

$$\oint_C \nabla\theta \cdot d\mathbf{r} = \pm 2\pi, \tag{B1}$$

where θ is the local phase. The line integral is taken over r around a closed curve C surrounding a local site. The sign of Eq.(B1) indicates the chirality; positive and negative signs correspond to clockwise and counterclockwise rotation, respectively. A spatial phase map was calculated for each frame of recorded data, and the phase singularities (PSs) are detected by checking the equality described above.

Acknowledgment

This work is partially supported by the JSPS, No. 24650147. The authors would like to thank Yusuke Uchiyama for useful comments.

References

[1] R. H. Clayton, et al. , Progr. Biophys. Molecul. Biol. **104** (2011) pp. 22-48.
[2] R. Harada and H. Konno, Pacific Science Review, **12** (2011) pp. 208-213.
[3] R. R. Aliev and A. V. Panfilov, Chaos, Soliton & Fractals, **7** (1996) pp. 293-301: $\dot{u} = -Ku(u-a)(u-1) - uv + D\nabla^2 u$ and $\dot{v} = (\epsilon + \mu_1 v/(\mu_2+u))(-\nu - Ku(u-b-1))$ with the parameters $a = 0.05$,$b = 0.1$,$K = 8.0$,$\epsilon = 0.01$,$\mu_1 = 0.07$, $\mu_2 = 0.3$ and $D = 1.0$.
[4] A. Suzuki and H. Konno, AIP Advances, **1** (2011) 032103 1-13.
[5] G. Beeler and H. Reuter, Reconstruction of the action potential of ventricular myocardial fibres, J. Physiol. 268, 177 (1977) pp. 177-210.
[6] H. Konno and P. Lomdahl, Stochastic Processes Having Fractional Order Nonlinearity Associated with Hyper Gamma Distribution, J. Phys. Soc. Jpn., **73** (2004) pp. 573-579.
[7] H. Konno, Advances in Mathematical Physics, **2010** (2010) 504267 1-12.
[8] W. Feller, Introduction to Probability Theory and Its Applications, Vol. I and II (Wiley, NY, 1967).
[9] Y. Ogata, J. Amer. Statist. Assoc., **83** (1988) pp. 9-27.
[10] C. W. Gardiner, Handbook of Stochastic Methods, (Springer, Berlin, 1983).
[11] L. Gil, J. Lega and J. M. Meunier, Phys. Rev. **A41** (1990) pp.1138-1141.
[12] K. E. Daniels and E. Bodenschatz, Phys. Rev. Lett. **88** (2002) 034501 1-4.
[13] C. Beta, A. S. Mikailov, H. H. Rotemund and G. Ertl, Europhys. Lett. **75** (2006) pp. 868-874.
[14] D. T. Gillespie, J. Phys. Chem. **81** (1977) pp.2341-2361.